Long-wave approximations in the description of bottom pressure

E. Didenkulova, E. Pelinovsky, Julien Touboul

Long-wave approximations in the description of bottom pressure

E. Didenkulova, E. Pelinovsky, Julien Touboul

Long-wave approximations in the description of bottom pressure

E. Didenkulova [a,*], E. Pelinovsky [a,b,c], J. Touboul [d]

[a] National Research University Higher School of Economics, Nizhny Novgorod, Russia
[b] Institute of Applied Physics of the Russian Academy of Sciences, Nizhny Novgorod, Russia
[c] Nizhny Novgorod State Technical University n.a. R.E Alekseev, Nizhny Novgorod, Russia
[d] Université de Toulon, Aix Marseille Univ., CNRS, IRD, MIO, Toulon, France

ARTICLE INFO

Article history:
Received 13 March 2020
Received in revised form 9 August 2020
Accepted 12 October 2020
Available online 14 October 2020

Keywords:
Bottom pressure
Korteweg–de Vries equation
Benjamin–Bona–Mahony equation
Whitham equation
Long wave
Rogue wave

ABSTRACT

The role of various long-wave approximations in the description of the wave field and bottom pressure caused by surface waves, and their relation to evolution equations are being considered. In the framework of the linear theory, these approximations are being tested on the well-known exact solution for the wave spectral amplitudes and pressure variations. The famous Whitham, Korteweg–de Vries (KdV) and Benjamin–Bona–Mahony (BBM) equations have been used as evolutionary equations. It has been shown that if the wave is long, though steep enough, the BBM approximation gives better results than the KdV approximation, and they are quite close to the exact results. The same applies to the description of rogue waves, though formed from smooth relatively long waves, are often short and steep, then they may be invisible in variations of the bottom pressure. Another advantage of the BBM approximation for calculating the bottom pressure is the ability to analyze noisy series without preliminary filtering, which is necessary when using the KdV approximation.

1. Introduction

Measuring sea waves using buoys in the coastal zone is a very difficult task for many reasons. The coastal buoy is heavily influenced by tipping waves and coastal currents. Many of them disappear due to vandalism of passing ships crews. That is why, the installation of bottom pressure sensors, which are easier to fix at the bottom and hide from vandals, has become a popular technology in measurements. For example, the DART (Deep-ocean Assessment and Reporting of Tsunamis) system is well-known for tsunami registration in the open ocean, which allows pre-registering a tsunami wave. In this case, however, an important practical problem of determining the elements of surface waves from variations in bottom pressure arises. This problem in the mathematical formulation belongs to the class of ill-posed problems, and although there are certain practical achievements, it is not considered to have been solved so far, as can be seen from engineering publications [1–8] and mathematical ones [9–17].

In our opinion, even in the direct correct problem of determining the bottom pressure under sea waves, there is still no complete clarity. Analytical formulas have been derived for a certain class of wave motions such as traveling waves in a basin of constant depth (such formulas can be found in the papers cited above), but they describe difficult integral expressions which are hard to make practical algorithms. The pressure formulas are explicit only in the long-wave

* Corresponding author.
E-mail address: eshurgalina@mail.ru (E. Didenkulova).

approximation in the framework of the highly nonlinear and weakly dispersive Green–Naghdi model [18,19]. They are used, for example, in the analytical calculation of bottom pressure under a solitary wave [20]. Numerical calculations of pressure under solitary waves are carried out in the framework of various models that demonstrate a certain difference in the results; see, for example, [21–23].

In this paper, we evaluate the role of long-wave approximations in estimating the characteristics of bottom pressure for modeling unsteady wave processes leading to the formation of rogue waves. All results are obtained analytically allowing investigating definition parameters of process. Evolution equations like Whitham, Korteweg–de Vries and Benjamin–Bona–Mahony equations are briefly discussed in Section 2. Long-wave approximations associated with these equations for the bottom pressure are derived in Section 3. Analytical calculations of bottom pressure induced by wave train focusing into the rogue wave are given in Section 4. The influence of the wave shape on the variation of bottom pressure is analyzed in Section 5. Bottom pressure induced by the focusing of frequency modulated (chirped) wave train is considered in Section 6 using the stationary-phase method. Obtained results are summarized in Conclusion.

2. The evolution equations for small amplitude surface waves

In the case of small-amplitude waves in a basin of constant depth, the original Euler equations can be exactly reduced to the Whitham equation in the linear approximation [24]

$$\frac{\partial \eta}{\partial t} + c_0 \int_{-\infty}^{+\infty} \hat{D}(x-y)\frac{\partial \eta(y,t)}{\partial y}dy = 0, \tag{1}$$

$$\hat{D}(\xi) = \frac{1}{2\pi}\int_{-\infty}^{+\infty} dk \sqrt{\frac{\tanh(kh)}{kh}}\exp(ik\xi). \tag{2}$$

Here $\eta(x,t)$ is the elevation of the free surface; h is the basin depth assumed to be constant; g is the acceleration of gravity; $c_0 = \sqrt{gh}$ is the speed of long waves; t is time, and x is the coordinate. This integral equation, actually, reflects the fact that the frequency of the monochromatic wave ω is related to the wave number k by the dispersion relation for surface gravity waves

$$\omega(k) = \sqrt{gk\tanh(kh)}. \tag{3}$$

In fact, the general solution of Eq. (1), as well as the original Euler equations, can be represented by the Fourier integral

$$\eta(x,t) = \frac{1}{2\pi}\mathrm{Re}\int_{-\infty}^{+\infty}\eta(k)\exp\{i[\omega(k)t - kx]\}dk, \tag{4}$$

where $\eta(k)$ is the Fourier spectrum of the wave determined by the initial condition

$$\eta(k) = \int_{-\infty}^{+\infty}\eta(x,0)\exp(ikx)dx. \tag{5}$$

In linear theory, of course, there is no difference between the application of evolution equations and the Fourier transform, but in the nonlinear problem, their difference becomes fundamental. Since our interest will be related to the calculation of bottom pressure, we will briefly first discuss the evolution equation (1) in various approximations.

We will focus on the relatively long waves that "reach" the bottom and can be detected by bottom pressure sensors. In the case of very long waves ($kh \ll 1$), the dispersion relation becomes very simple

$$\omega(k) = c_0 k, \tag{6}$$

and the Whitham equation is reduced to the transport equation

$$\frac{\partial \eta}{\partial t} + c_0\frac{\partial \eta}{\partial x} = 0, \tag{7}$$

its solution is trivial

$$\eta(x,t) = \eta_0(x - c_0 t). \tag{8}$$

This is a well-known solution of linear shallow water equations that we will not discuss further.

Accounting for the next correction in kh leads to the modification of the dispersion relation (6)

$$\omega = c_0 k\left(1 - \frac{k^2h^2}{6}\right), \tag{9}$$

and the transformation of the Whitham equation into a differential equation

$$\frac{\partial \eta}{\partial t} + c_0\frac{\partial \eta}{\partial x} + \frac{c_0h^2}{6}\frac{\partial^3 \eta}{\partial x^3} = 0. \tag{10}$$

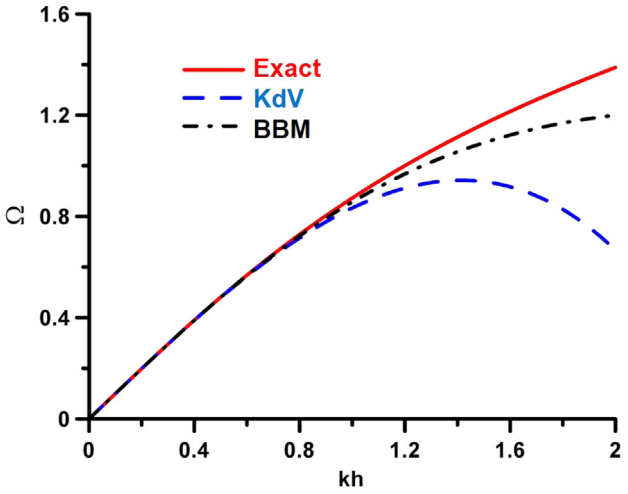

Fig. 1. Different approximations of the dispersion relation for surface gravity waves.

This is a linear approximation of the well-known Korteweg–de Vries (KdV) equation, which played a crucial role in the nonlinear theory of water waves, in particular for describing solitons.

With the same accuracy (like $\frac{1}{1+\varepsilon} \approx 1-\varepsilon, \varepsilon \ll 1$), we can propose another approximation of the dispersion relation

$$\omega = \frac{c_0 k}{1+\frac{k^2h^2}{6}}, \tag{11}$$

leading to the next transformation of the Whitham equation

$$\frac{\partial \eta}{\partial t} + c_0 \frac{\partial \eta}{\partial x} - \frac{h^2}{6}\frac{\partial^3 \eta}{\partial t \partial x^3} = 0, \tag{12}$$

which is known as the linear part of the Benjamin–Bona–Mahony — BBM equation [25]. It is not integrable as the Korteweg–de Vries equation, and is not actually used in the practice of calculating water waves.

The accuracy of various long-wavelength dispersion approximations is illustrated in Fig. 1. Here $\Omega = \omega\sqrt{h/g}$ is the dimensionless frequency. As we see in the range $kh \sim 1$, the long-wave approximations coincide well with the exact curve. In the short-wave region, the differences are more significant, especially in the case of the KdV approximation. This difference can affect long waves due to nonlinear interactions; in the linear approximation the difference affect the convergence of solutions. In principle, it is possible to find the long-wave approximation of the dispersion relation using the *Padé* decomposition, which can expand the coincidence region [26]. In the simple variant, it is a combination of Eqs. (10) and (12); it has been considered, for example, in [27]. However, we restrict here to the analysis of the long-wave approximation in the framework of the KdV and BBM equations.

3. Bottom pressure caused by surface waves — long-wave approximations

It is convenient to measure the bottom pressure through the so-called displacement of the mercury column:

$$p = \rho g(h+\xi), \tag{13}$$

where ρ is the density of sea water. Then from the linearized equations of hydrodynamics we obtain the following relationship between the spectra of bottom pressure and displacement of the water surface [28]

$$\xi(k) = \frac{\eta(k)}{\cosh(kh)}. \tag{14}$$

Using the direct Fourier transform, we can obtain the integral relationship between the bottom pressure and the displacement of the water surface. However, in practice it is easier to use direct and inverse Fourier transforms. The function $1/\cosh(kh)$ is a transfer function, or rather its spectrum. Similar transfer function is appeared in the problems of tsunami generation by the instantaneous vertical motion of the sea bottom [29].

Formula (14) implies the well-known fact that short waves do not reach the seabed and cannot lead to changes in bottom pressure. Therefore, the main attention is paid to waves of large and moderate lengths (compared to the depth

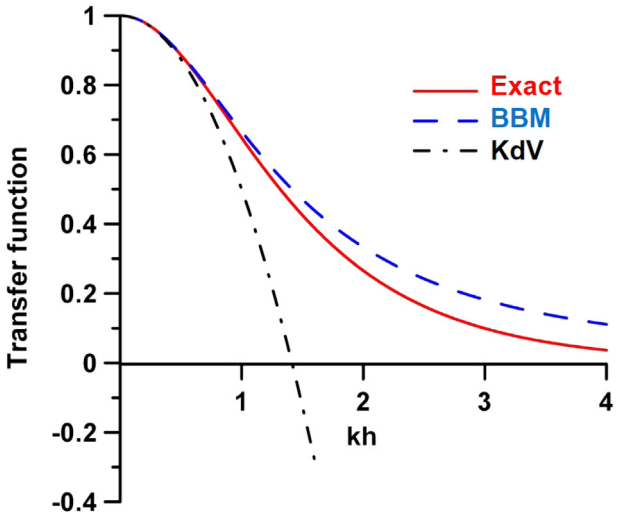

Fig. 2. Various approximations of the transfer function.

of the basin. In this case, by analogy with the results of the previous section, we can expand the transfer function in a Taylor series, limiting by two terms, rewrite (14) approximately in the form

$$\xi_{KdV}(k) \approx \left[1 - \frac{k^2h^2}{2}\right]\eta(k). \tag{15}$$

Here we have used the abbreviation KdV, since the same decomposition is used to derive the Korteweg–de Vries equation (9). In this case, the direct Fourier transform leads to an explicit formula for bottom pressure variations

$$\xi(x) = \eta(x) + \frac{h^2}{2}\frac{d^2\eta}{dx^2}. \tag{16}$$

In this approximation, there are no residual variations in bottom pressure after the passage of the sea wave. It is important to note, it is the formula (16) that constitutes the linear part of the bottom pressure in the framework of the weakly dispersed strongly nonlinear Green–Naghdi model [6,22], which is actively used to calculate sea waves in the coastal zone. Essentially, our conclusion shows where such a term comes from.

With the same accuracy, the transfer function in the region of long waves can be represented in the form:

$$\xi_{BBM}(k) \approx \frac{\eta(k)}{1 + \frac{k^2h^2}{2}}, \tag{17}$$

where we use the abbreviation BBM, since such an expansion is used in (11). Applying the direct Fourier transform to (17), we obtain a differential equation for the spatial distribution of bottom pressure:

$$\xi(x) - \frac{h^2}{2}\frac{d^2\xi}{dx^2} = \eta(x). \tag{18}$$

This equation is easily solved:

$$\xi(x) = \frac{\sqrt{2}}{h}\int_0^x \eta(y)\sin h\left(\sqrt{2}\frac{y-x}{h}\right)dy \tag{19}$$

and it is convenient for numerical integration.

Thus, there are two long-wavelength approximations of the transfer function, and their accuracy is illustrated in Fig. 2. As we see, in the region of very long waves ($kh \ll 1$) the curves coincide. The BBM approximation (6) is close to the exact curve to approximately $kh \sim 2$, and qualitatively coincides with it in the entire range of wave numbers. The KdV approximation (9) seems to be the worst, since the transfer function in the region $kh > 1.42$ becomes negative and grows strongly for short waves, contrary to the well-known fact that short waves do not reach the bottom. It underlines the modern Green–Naghdi models for describing long water waves.

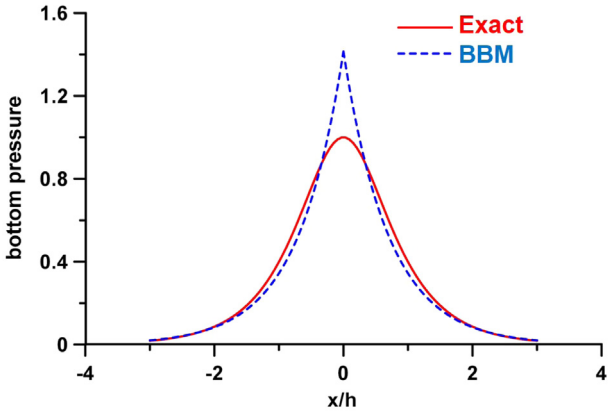

Fig. 3. The profile of the bottom "ideal" rogue wave. Solid red line — exact (Eq. (21)) and dashed blue line — BBM (Eq. (22)).

4. Rogue wave image in bottom pressure variations

We will demonstrate the difference in the predictions of various models using the example of an "ideal" rogue wave in the form of a delta-function

$$\eta(x) = A_0\delta(x/l), \tag{20}$$

where the amplitude and length parameters have been introduced only for dimension. Such a wave satisfies all the criteria of a rogue wave, since it significantly exceeds all possible surrounding waves in amplitude [30]. Its spectrum is $A_0 l_0$ and the direct Fourier transform using the exact transfer function (14) gives an answer [31, Eq. 3.981.3]:

$$\xi(x) = \pi A_0 \frac{l}{h}\operatorname{sech}\left(\frac{\pi x}{2h}\right). \tag{21}$$

As can be seen, the "bottom rogue wave" looks like a short smooth pulse (its length is of the order of depth), and the amplitude depends on the ratio between the "initial" length and depth.

Similar calculations with the BBM approximation of the transfer function lead to [31, Eq. 3.723.2]

$$\xi(x) = \pi\sqrt{2}A_0 \frac{l}{h}\exp\left(-\sqrt{2}\frac{|x|}{h}\right). \tag{22}$$

We do not use the KdV approximation (15), since the corresponding integrals and functions diverge. A comparison of formulas (21) and (22) is shown in Fig. 3 (normalized amplitude). As expected, the BBM approximation overestimates the amplitude of the bottom pressure and does not prevent the formation of a singularity in the profile (jump in the derivative), the value of which decreases with the increasing depth of the basin.

5. Single wave image in bottom pressure variations

Obviously, an "ideal" wave is short, and it is natural to expect that long-wave approximations would not work. Nevertheless, as we see from Fig. 3, the BBM approximation describes well the form of pressure variations, although it greatly overestimates the value of bottom pressure. Let us therefore consider a more realistic case of a long wave of a rectangular shape (this choice is due to the receipt of analytical expressions)

$$\eta_0(x) = A_0\begin{cases}1 & -l < x < l\\ 0 & \text{out of interval}\end{cases} \tag{23}$$

Then an exact expression for the bottom pressure is in the form [31, Eq. 4.122.1]

$$\xi(x) = \frac{2A_0}{\pi}\operatorname{atan}\left[\frac{\sinh(\pi l/2h)}{\cosh(\pi x/2h)}\right]. \tag{24}$$

Similar calculations using the BBM approximation lead to the following expression [31, Eq. 3.725.3]

$$\xi_{BBM}(x) = A_0\begin{cases}1-\cosh(\sqrt{2}x/h)\exp(-\sqrt{2}l/h) & |x| < l\\ \sinh(\sqrt{2}l/h)\exp(-\sqrt{2}x/h) & |x| > l\end{cases} \tag{25}$$

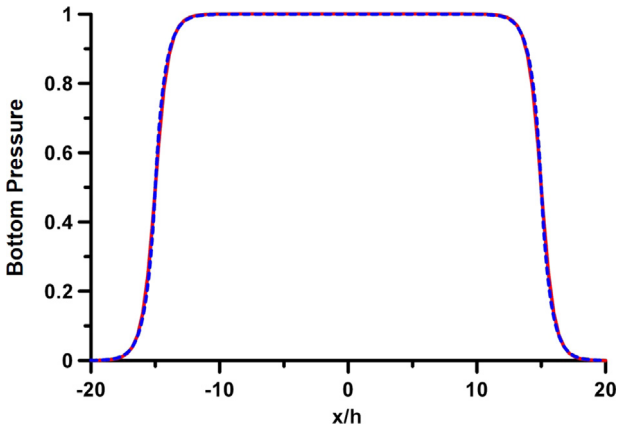

Fig. 4. The response of a long wave of a rectangular shape in variations of the bottom pressure (the solid red curve is the exact solution, and the dashed blue line is the BBM approximation), $l/h = 15$.

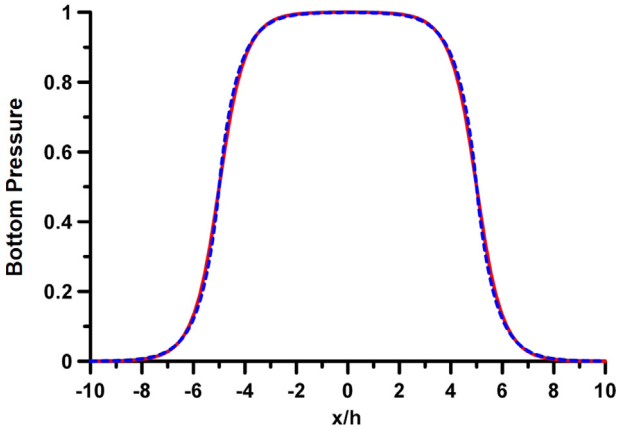

Fig. 5. The response of a long wave of a rectangular shape in variations of the bottom pressure (the solid red curve is the exact solution, and the dashed blue line is the BBM approximation), $l/h = 2$.

These dependences are presented in Fig. 4 for the case of a long wave $l/h = 15$ (the amplitude is normalized to A_0). As expected, the pressure in the long wave is hydrostatic, but on the wave slopes it decreases sharply. In this case, the BBM approximation comes up to the form of pressure variations very well, so it can be used even if there are sections with a large steepness in the wave field. The KdV approximation cannot describe an impulse with sharp slopes, and then endless surges appear in pressure.

Even if the wave is not very long ($l/h = 2$), the BBM approximation still works well (Fig. 5), although the difference in pressure from hydrostatics becomes noticeable and the shape of the pressure variations differs significantly from a rectangular one.

The last analytical example in this section is a smooth pulse on the surface with small oscillations at the edges

$$\eta(x) = A_0 \left[1 + \left(\frac{h}{l}\right)^2 - \frac{2h^2x^2}{l^4} \right] \exp\left[-\left(\frac{x}{l}\right)^2 \right]. \tag{26}$$

In this case, calculations of the bottom pressure in the long-wave approximation result in the following expressions:

$$\xi_{BBM}(x) = A_0 \exp\left[-\left(\frac{x}{l}\right)^2 \right], \tag{27}$$

$$\xi_{KdV}(x) = A_0 \left[1 - \frac{3h^4}{l^4} + \frac{12h^4x^2}{l^6} - \frac{4h^4x^4}{l^8} \right] \exp\left[-\left(\frac{x}{l}\right)^2 \right]. \tag{28}$$

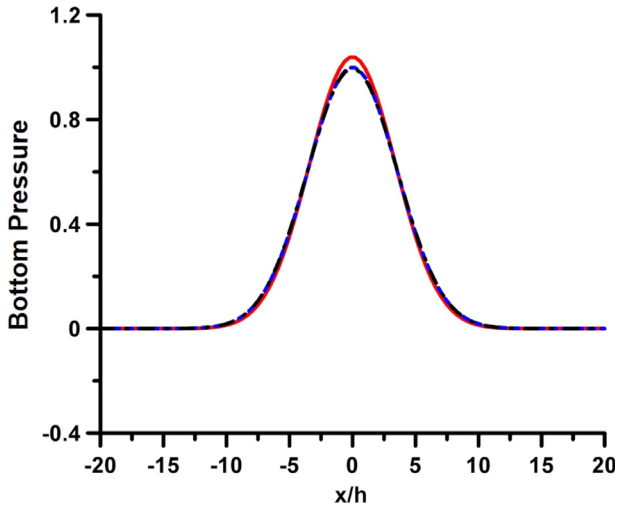

Fig. 6. The response of a long wave of a smooth shape in variations of the bottom pressure (solid red curve is a surface displacement, dashed blue curve is the BBM approximation, and dashed dotted black curve is the KdV approximation), $l/h = 5$.

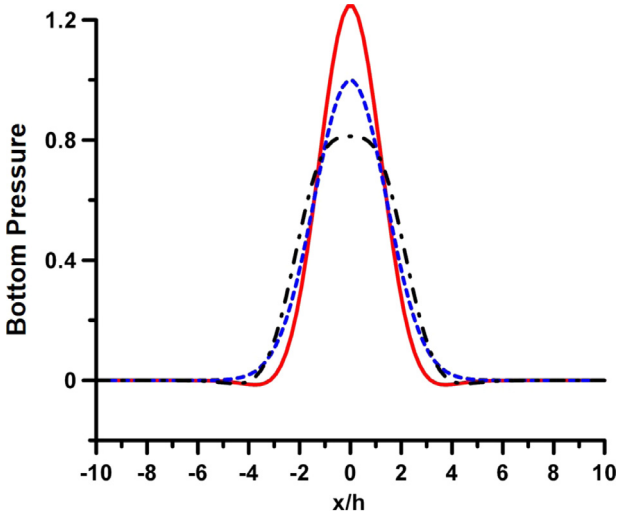

Fig. 7. The response of a long wave of a smooth shape in variations of the bottom pressure (solid red curve is a surface displacement, dashed blue curve is the BBM approximation, and dashed dotted black curve is the KdV approximation), $l/h = 2$.

If the wave is very long ($l/h = 5$), then the difference in predictions of the BBM and KdV models is insignificant (Fig. 6), which could be expected for waves whose entire spectrum is concentrated in long waves. However, for shorter waves ($l/h = 2$), the difference becomes noticeable (Fig. 7).

6. Dispersion focusing of frequency-modulated wave packets

The dispersive compression of frequency-modulated packets is one of the mechanisms of rogue wave formation [30] and is often used in laboratory tanks to generate large-amplitude pulses. For this, there must be an optimal distribution of spectral components in space, described by a self-similar solution to the kinematic equation [24,30]:

$$c_{gr}[k(x,t)] = \frac{d\omega}{dk} = \frac{x_f - x}{t_f - t}, \tag{29}$$

or close to it. Here x_f is the position of the focal point at which all wave packets converge at time t_f. Having the initial distribution of the wave number at $t = 0$ in accordance with (29), one may be sure that the rogue wave will be the largest. The problem, however, is that having "organized" the optimal focusing within the framework of the exact equations of hydrodynamics, we will not be able to reproduce it in the framework of long-wavelength models. Indeed, the group

velocity for surface waves is always positive; while in the KdV and BBM models it is negative for short waves. It is natural, therefore, to be limited to the values of $kh \sim 1$, when the differences in the approximations of the dispersion relation have not yet become crucial. It is quite difficult to solve the problem of focusing a frequency-modulated (chirped) wave packet, however, you can use the invariance property of the hydrodynamic equations with respect to the change of signs of time and coordinate, and solve the problem of transforming a rogue wave into a frequency-modulated packet, and then invert it in space. This technique has been used in a number of works [30,32]. Choosing, for example, a rogue wave in the form of a Gaussian pulse:

$$\eta_0(x) = A_0 \exp\left(-\frac{x^2}{l^2}\right), \tag{30}$$

it is easy to calculate the structure of the wave packet at large times using the stationary phase method [33]

$$\eta(x,t) = A[x,t;k_*(x,t)]\cos\left[\omega(k_*)t - k_* x - \pi/4\right], \tag{31}$$

where the envelope of the wave packet is

$$A[x,t;k_*(x,t)] = A_0 l\sqrt{\frac{2}{t|d^2\omega/dk^2|}}\exp\left(-\frac{k_*^2 l^2}{4}\right), \tag{32}$$

and

$$c_{gr}[k_*(x,t)] = \frac{d\omega}{dk} = \frac{x}{t}. \tag{33}$$

The nature of the amplitude distribution over the spectrum is determined by the function (the normalizations are the same as in Fig. 1, and $K = kh$):

$$F(K) = \frac{1}{\sqrt{|d^2\Omega/dK^2|}}\exp\left[-\frac{K^2}{4}\left(\frac{l}{h}\right)^2\right]. \tag{34}$$

In particular, in the KdV approximation spectral amplitude is

$$F_{KdV}(K) = \frac{1}{\sqrt{K}}\exp\left[-\frac{K^2}{4}\left(\frac{l}{h}\right)^2\right]. \tag{35}$$

In BBM approximation the amplitude function is

$$F_{BBM}(K) = \frac{(1+K^2/6)^{3/2}}{\sqrt{K\left|1-K^2/18\right|}}\exp\left[-\frac{K^2}{4}\left(\frac{l}{h}\right)^2\right]. \tag{36}$$

Functions (35) and (36) are shown in Fig. 8 for the case $l/h = 2$. As we see, the curves differ from each other, but not too much for $kh < 2$. The spectral amplitudes of bottom pressure variations have been obtained from (34) using the transfer function in various approximations. In particular, the bottom pressure spectral amplitudes are

$$P_{KdV}(K) = F_{KdV}(K)\left|1-\frac{K^2}{2}\right|, \tag{37}$$

$$P_{BBM}(K) = \frac{F_{BBM}(K)}{1+\frac{K^2}{2}}. \tag{38}$$

These functions are presented in Fig. 9. Here the difference between KdV and BBM approximations is more visible.

As it is known, the stationary phase method is not valid in the vicinity of the leading wave where the wavenumber values are small. This problem has been analyzed in [34] with use of the exact dispersion relation and it was shown that leading wave amplitude is bounded. In the KdV approximation, the leading wave is described by the Airy function and this solution is given in many books on nonlinear waves. The difference in results is small on large times. The same is expected for BBM approximation of the dispersion relation. Inversing the wave field in space we obtain the focusing of weak chirped wave train in the rogue wave of Gaussian shape (30). If its amplitude is large and length is small (almost "ideal" rogue wave), it will be manifested in the bottom pressure variations as a small signal, see Section 4.

7. Conclusion

The applicability of various long-wave approximations has been investigated in the description of the wave field and bottom pressure caused by surface waves. Within the framework of linear theory, an exact formula that relates the spectral amplitudes of a wave and pressure variations, which allows testing long-wave approximations is known. We

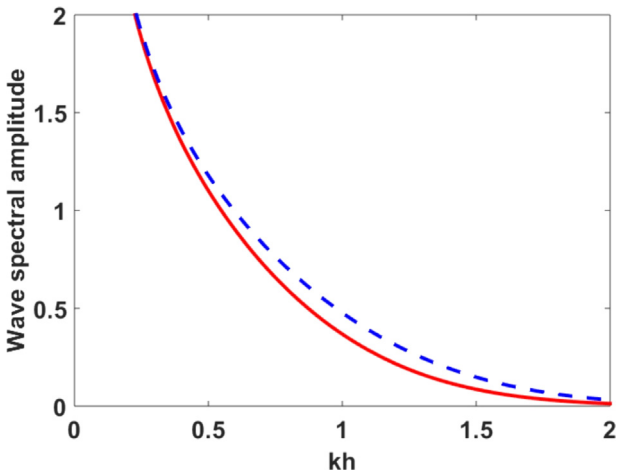

Fig. 8. Normalized spectral amplitudes of the wave field at $l/h = 2$. The solid red line is the KdV and the dashed blue line is the BBM approximation.

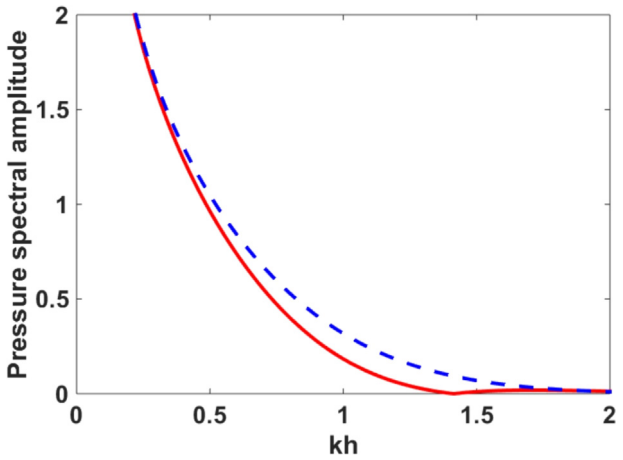

Fig. 9. The normalized spectral amplitudes of pressure variations at $l/h = 2$. The solid red line is the KdV and the dashed blue line is the BBM approximation.

show how these formulas are related to the well-known evolution equations used in the theory of water waves. Exactly propagating waves are described by the Whitham equation in the linear approximation, while the Korteweg–de Vries (KdV) and Benjamin–Bona–Mahony (BBM) equations are used in the long-wave approximation. In the framework of these approximations, the bottom pressure can be calculated using simple differentiation and integration operations without using the Fourier transform, which requires a sufficiently long record. The obvious fact is demonstrated that if the wave is long and sufficiently smooth ($kh \sim 1$), both long-wave approximations provide sufficient accuracy and there is no particular difference in the use of one or another approximation. However, if the wave is long, though steep enough, the BBM approximation gives better results than the KdV one, and is quite close to the exact results. The same relates to the description of rogue waves, though formed from smooth relatively long waves, are often short and steep. Another advantage of the BBM approximation for calculating the bottom pressure is the ability to analyze noisy series without preliminary filtering, which is necessary when using the KdV approximation. It is important to note that in the existing highly nonlinear models of wave movements in the coastal zone, the KdV approximation (in the linear approximation) is used to calculate the pressure; so the question of the "correct" formula for pressure is not solved yet. Finally, the important conclusion that follows from our analysis is that, although the BBM approximation works well in almost the entire range of wave numbers, it results in small bottom pressures if the rogue wave is relatively short and steep (the same conclusion follows from the exact solution). Therefore, it is still unclear how correctly to distinguish rogue waves from bottom pressure records.

CRediT authorship contribution statement

E. Didenkulova: Investigation, Writing - review & editing, Methodology. **E. Pelinovsky:** Conceptualization, Writing - original draft. **J. Touboul:** Investigation, Writing - review & editing.

Declaration of competing interest

The authors declare that they have no known competing financial interests or personal relationships that could have appeared to influence the work reported in this paper.

Acknowledgments

This work is done within the joint Russian–French grant (RFBR No 19-55-15005). Particular support from the RFBR grants (20-05-00162 and 18-05-80019) and the grant for state support of scientific research of leading scientific schools of the RF (NSh-2485.2020.5) is also acknowledged. The CNRS is greatly acknowledged for the French part of the Russian–French grant.

References

[1] L. Cavaleri, Wave measurement using pressure transducer, Oceanol. Acta 3 (1980) 339–345.
[2] H. Wang, D.Y. Lee, A. Garcia, Time series surface-wave recovery from pressure gage, Coast. Eng. 10 (1986) 379–393.
[3] C. Bishop, M. Donelan, Measuring waves with pressure transducers, Coast. Eng. 11 (1987) 309–328.
[4] A. Baqueizo, M.A. Losada, Transfer function between wave height and wave pressure for progressive waves, Coast. Eng. 24 (1995) 351–353, http://dx.doi.org/10.1016/0378-3839(94)00038-Y.
[5] M. Zaslavsky, V. Krasitsky, About recovery of surface wave spectrum from pressure sensor, Oceanology 41 (2001) 195–200.
[6] P. Bonneton, D. Lannes, K. Martins, H. Michallet, A nonlinear weakly dispersive method for recovering the elevation of irrotational surface waves from pressure measurements, Coast. Eng. 138 (2018) 1–8, http://dx.doi.org/10.1016/j.coastaleng.2018.04.005.
[7] K. Martins, P. Bonneton, A. Mouragues, B. Castelle, Non-hydrostatic, non-linear processes in the surf zone, J. Geophys. Res.: Oceans 125 (2020) e2019JC015521, http://dx.doi.org/10.1029/2019JC015521.
[8] C.-H.Tsai M.-C. Huang, F.-J. Young, et al., On the recovery of surface wave by pressure transfer function, Ocean Eng. 32 (2005) 1247–1259, http://dx.doi.org/10.1016/j.oceaneng.2004.10.020.
[9] J. Esher, T. Schlurmann, On the recovery of the free surface from the pressure within periodic travelling water waves, J. Nonlinear Math. Phys. 15 (2008) 50–57, http://dx.doi.org/10.2991/jnmp.2008.15.s2.4.
[10] B. Deconink, K. Olivears, V. Vasan, Relating the bottom pressure and surface elevation in the water wave problem, J. Nonlinear Math. Phys. 19 (2012) 1240014, http://dx.doi.org/10.1142/S1402925112400141.
[11] A. Constantin, On the recovery of solitary wave profiles from pressure measurements, J. Fluid Mech. 669 (2012) 376–384, http://dx.doi.org/10.1017/jfm.2012.114.
[12] K.L. Oliveras, V. Vasan, B. Deconick, et al., Recovering surface elevation from pressure data, SIAM J. Appl. Math. 72 (2012) 897–918.
[13] D. Clamond, A. Constantin, Recovery of steady periodic wave profiles from pressure measurements at the bed, J. Fluid Mech. 714 (2013) 463–475, http://dx.doi.org/10.1017/jfm.2012.490.
[14] H.-C. Hsu, Recovering surface profiles of solitary waves on a uniform stream from pressure measurements, Discrete Contin. Dyn. Syst. 34 (2014) 3035–3043, http://dx.doi.org/10.3934/dcds.2014.34.3035.
[15] V. Vasan, K.L. Oliveras, Water-wave profiles from pressure measurements: Extensions, Appl. Math. Lett. 68 (2017) 175–180, http://dx.doi.org/10.1016/j.aml.2017.01.017.
[16] V. Vasan, K. Oliveras, D. Henderson, B. Deconinck, A method to recover water-wave profiles from pressure measurements, Wave Motion 75 (2017) 25–35, http://dx.doi.org/10.1016/j.wavemoti.2017.08.003.
[17] P. Bonneton, D. Lannes, Recovering water wave elevation from pressure measurements, J. Fluid Mech. 833 (2017) 399–429, http://dx.doi.org/10.1017/jfm.2017.666.
[18] A.E. Green, P.M. Naghdi, A derivation of equations for wave propagation in water of variable depth, J. Fluid Mech. 78 (1976) 237–246.
[19] E. Barthelemy, Nonlinear shallow water theories for coastal waves, Surv. Geophys. 25 (2004) 315–337, http://dx.doi.org/10.1007/s10712-003-1281-7.
[20] E.N. Pelinovsky, K.I. Kuznetsov, J. Touboul, A.A. Kurkin, Bottom pressure caused by passage of a solitary wave within the strongly nonlinear green–naghdi model, Dokl. Phys. 60 (2015) 171–174, http://dx.doi.org/10.1134/S1028335815040035.
[21] J. Touboul, E. Pelinovsky, On the use of linear theory for measuring surface waves using bottom pressure distribution, Eur. J. Mech. – B: Fluids 67 (2018) 97–103, http://dx.doi.org/10.1016/j.euromechflu.2017.08.007.
[22] J. Touboul, E. Pelinovsky, Bottom pressure distribution under a solitonic wave reflecting on a vertical wall, Eur. J. Mech. B Fluids 48 (2014) 13–18, http://dx.doi.org/10.1016/j.euromechflu.2014.03.011.
[23] A. Slunyaev, E. Pelinovsky, H.-C. Hsu, The pressure field beneath intense surface water wave groups, Eur. J. Mech. B/Fluids 67 (2018) 25–34, http://dx.doi.org/10.1016/j.euromechflu.2017.08.002.
[24] G.B. Whitham, Linear and Nonlinear Waves, John Wiley Sons, New York, 1974.
[25] T.B. Benjamin, J.L. Bona, J.J. Mahony, Model equations for long waves in nonlinear dispersive systems, Philos. Trans. R. Soc. London, Ser. A 272 (1972) 47–78.
[26] P.A. Madsen, H.B. Bingham, H.A. Schäffer, Boussinesq-Type formulations for fully nonlinear and extremely dispersive water waves: derivation and analysis, Proc. R. Soc. Lond. A 459 (2003) 1075–1104, http://dx.doi.org/10.1098/rspa.2002.1067.
[27] M. Francius, E. Pelinovsky, A. Slunyaev, Wave dynamics in nonlinear media with two dispersionless limits for long and short waves, Phys. Lett. A 280 (2001) 53–57, http://dx.doi.org/10.1016/S0375-9601(01)00042-1.
[28] C.C. Mei, Applied Ocean Surface Waves, World Scientific, Singapore, 1989.
[29] C.-M. Liu, Analytical solutions of tsunamis generated by underwater earthquakes, Wave Motion 93 (2020) 102489, http://dx.doi.org/10.1016/j.wavemoti.2019.102489.
[30] Ch. Kharif, E. Pelinovsky, A. Slunyaev, Rogue Waves in the Ocean, Springer, Berlin, 2009.
[31] I.S. Gradshteyn, I.M. Ryzhik, Table of Integrals, Series, and Products, Elsevier, Amsterdam, 2007.
[32] A. Chabchoub, M. Fink, Time-reversal generation of rogue waves, Phys. Rev. Lett. 112 (2014) 124101, http://dx.doi.org/10.1103/PhysRevLett.112.124101.
[33] R. Wong, Asymptotic Approximations of Integrals, in: Classics in Applied Mathematics, vol. 34, SIAM, Philadelphia, 2001.
[34] Yu.L. Gazaryan, About surface waves in the ocean generated by underwater earthquakes, Sov. Phys. Acoust. 1 (1955) 203–217.